

**Search for the charge-conjugation-forbidden decay  $\omega \rightarrow \eta\pi^0$** 

A. Starostin,<sup>1,\*</sup> B. M. K. Nefkens,<sup>1</sup> J. Ahrens,<sup>2</sup> J. R. M. Annand,<sup>3</sup> H. J. Arends,<sup>2</sup> K. Bantawa,<sup>4</sup> P. A. Bartolome,<sup>2</sup> R. Beck,<sup>2,5</sup> V. Bekrenev,<sup>6</sup> A. Braghieri,<sup>7</sup> D. Branford,<sup>8</sup> W. J. Briscoe,<sup>9</sup> J. Brudvik,<sup>1</sup> S. Cherepnaya,<sup>10</sup> E. J. Downie,<sup>2,3</sup> L. V. Filkov,<sup>10</sup> D. I. Glazier,<sup>8</sup> R. Gregor,<sup>11</sup> E. Heid,<sup>2</sup> D. Hornidge,<sup>12</sup> O. Jahn,<sup>2</sup> T. C. Jude,<sup>8</sup> V. L. Kashevarov,<sup>10</sup> R. Kondratiev,<sup>13</sup> M. Korolija,<sup>14</sup> M. Kotulla,<sup>11</sup> A. Koulbardis,<sup>6</sup> S. Kruglov,<sup>6</sup> B. Krusche,<sup>15</sup> V. Lisin,<sup>13</sup> K. Livingston,<sup>3</sup> I. J. D. MacGregor,<sup>3</sup> Y. Maghrbi,<sup>15</sup> D. M. Manley,<sup>4</sup> M. Martinez,<sup>2</sup> J. C. McGeorge,<sup>3</sup> E. F. McNicoll,<sup>3</sup> D. Mekterovic,<sup>14</sup> V. Metag,<sup>11</sup> S. Micanovic,<sup>14</sup> M. Ostrick,<sup>2</sup> P. Pedroni,<sup>7</sup> F. Pheron,<sup>15</sup> A. Polonski,<sup>13</sup> S. Prakhov,<sup>1</sup> J. Robinson,<sup>3</sup> G. Rosner,<sup>3</sup> M. Rost,<sup>2</sup> S. Schumann,<sup>2,5</sup> M. H. Sikora,<sup>8</sup> D. Sober,<sup>16</sup> I. M. Suarez,<sup>1</sup> I. Supek,<sup>14</sup> C. M. Tarbert,<sup>8</sup> M. Thiel,<sup>11</sup> A. Thomas,<sup>2</sup> M. Unverzagt,<sup>2,5</sup> and D. P. Watts<sup>8</sup>

(Crystal Ball Collaboration at MAMI)

<sup>1</sup>*University of California Los Angeles, Los Angeles, California 90095-1547, USA*

<sup>2</sup>*Institut für Kernphysik, University of Mainz, D-55099 Mainz, Germany*

<sup>3</sup>*Department of Physics and Astronomy, University of Glasgow, Glasgow G12 8QQ, United Kingdom*

<sup>4</sup>*Kent State University, Kent, Ohio 44242-0001, USA*

<sup>5</sup>*Helmholtz-Institut für Strahlen-und Kernphysik, University of Bonn, D-53115 Bonn, Germany*

<sup>6</sup>*Petersburg Nuclear Physics Institute, RU-188350 Gatchina, Russia*

<sup>7</sup>*INFN Sezione di Pavia, I-27100 Pavia, Italy*

<sup>8</sup>*School of Physics, University of Edinburgh, Edinburgh EH9 3JZ, United Kingdom*

<sup>9</sup>*The George Washington University, Washington, D. C. 20052, USA*

<sup>10</sup>*Lebedev Physical Institute, RU-119991 Moscow, Russia*

<sup>11</sup>*II Physikalisches Institut, University of Giessen, D-35392 Giessen, Germany*

<sup>12</sup>*Mount Allison University, Sackville, New Brunswick E4L 3B5, Canada*

<sup>13</sup>*Institute for Nuclear Research, RU-117312 Moscow, Russia*

<sup>14</sup>*Rudjer Boskovic Institute, Zagreb 10002, Croatia*

<sup>15</sup>*Institut für Physik, University of Basel, CH-4056 Basel, Switzerland*

<sup>16</sup>*The Catholic University of America, Washington, D. C. 20064, USA*

(Received 9 December 2008; published 4 June 2009)

A new upper limit of  $2.3 \times 10^{-4}$  on the branching ratio of the decay  $\omega \rightarrow \eta\pi^0$  has been obtained using the Crystal Ball multiphoton spectrometer at the Mainz Microtron MAMI. This decay is forbidden by charge-conjugation invariance of the strong and electromagnetic interactions. We have also obtained the upper limit of  $2.3 \times 10^{-4}$  for the forbidden decay  $\omega \rightarrow 3\pi^0$  and the upper limit of  $2.4 \times 10^{-4}$  for  $\omega \rightarrow 2\pi^0$ .

DOI: [10.1103/PhysRevC.79.065201](https://doi.org/10.1103/PhysRevC.79.065201)

PACS number(s): 11.30.Er, 13.25.Jx, 14.40.Cs

Breaking charge-conjugation symmetry is one of the three Sakharov conditions required for explaining the mysterious excess of matter over antimatter in the known universe [1]. An experimental observation of violation of charge-conjugation symmetry in strong or electromagnetic interactions would indicate physics outside the standard model [2]. The “Review of Particle Physics” [3] lists 206 tests of  $CP$ , but only 22 tests of charge-conjugation (or  $C$ ) invariance. Half of these are electromagnetic transitions; their sensitivity is down by  $\alpha$ . 11 of the tests of  $C$  are  $\eta$  decays, seven are decays of  $\eta'$ , two are  $\omega$ , one is a  $\pi^0$  decay, and one is a decay of  $J/\psi$ . In this article we report on a new experiment to search for  $C$ -violation in  $\omega \rightarrow \eta\pi^0$  decay. The existing upper limit,  $BR(\omega \rightarrow \eta\pi^0) < 1 \times 10^{-3}$ , was obtained by the GAMS2000 Collaboration [4]. They used a 38 GeV/ $c$   $\pi^-$  beam to produce the  $\omega$  mesons. Our experiment uses a photon beam for  $\omega$  production near threshold. We also report new upper limits on the branching ratios for  $\omega \rightarrow 3\pi^0$  and  $\omega \rightarrow 2\pi^0$ . The  $\omega \rightarrow 3\pi^0$  decay is listed in Ref. [3] as another test of  $C$ . The current upper limit,  $BR(\omega \rightarrow 3\pi^0) < 3 \times 10^{-4}$ , was also

obtained by GAMS2000 [5]. The decay  $\omega \rightarrow 2\pi^0$  is forbidden by the Bose-Einstein statistics constraint. No measurement of this decay has been reported.

The experiment was conducted at the Mainz Microtron Facility using a secondary beam of tagged photons produced by the 1.5 GeV electron accelerator MAMI-C. The energy of the photons in the beam was measured to an accuracy of 3–4 MeV by the Glasgow photon tagger [6–8]. The maximum energy of the tagged photon beam available in the experiment was 1.403 GeV. The experimental setup consists of the large-acceptance electromagnetic spectrometer Crystal Ball (CB) equipped with the TAPS detector as a forward wall. The Crystal Ball is a highly segmented detector made of 672 NaI triangular-pyramidal crystals about 16 radiation length (r.l.) long, assembled into two hemispheres. There are two  $21^\circ$  openings, one at the beam-entrance and the other at the beam-exit side of the detector. A spherical cavity in the center of the detector is used to house the liquid hydrogen target and a particle identification detector (PID). The PID detector surrounding the liquid hydrogen target is made of 24 strips of plastic scintillator 50 cm long and 4 mm thick. Although the Crystal Ball is optimized for the detection of photons and electrons, it has also good efficiency

\*starost@ucla.edu

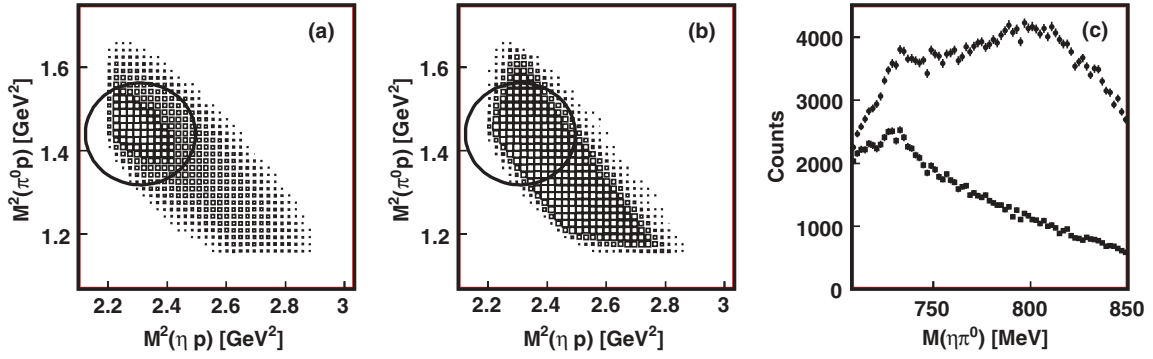


FIG. 1. (a) Experimentally observed Dalitz plot for the reconstructed  $\gamma p \rightarrow \eta\pi^0 p$  events integrated over the beam energies from 1.171 GeV to 1.322 GeV. The black circle on the plot indicates the two dimensional cut applied to the event sample before calculating the  $\omega \rightarrow \eta\pi^0$  upper limit. (b) The same distribution obtained for the reconstructed  $\gamma p \rightarrow \omega(\eta\pi^0)p$  Monte Carlo events. (c) Invariant mass of  $\eta\pi^0$  before (solid circles) and after (solid squares) the cut on the  $\gamma p \rightarrow \eta\pi^0 p$  Dalitz plot.

for detecting neutrons and protons. See Refs. [9–11] for details.

In its current configuration, TAPS [12,13] comprises 384 individual barium fluoride (BaF<sub>2</sub>) crystals arranged in the form of a hexagonal prism. Each TAPS crystal has the shape of a hexagon with an inscribed diameter of 59 mm and length 250 mm (12 r.l.). One crystal in the center of the TAPS detector has been removed allowing the beam to exit. The TAPS detector is located 147.5 cm downstream of the center of the CB and covers the range in polar angle approximately between 1° and 20°. The combination of CB and TAPS detectors covers ≈97% of the solid angle.

The  $\gamma p \rightarrow \eta\pi^0 p$  events produced in a 5 cm-long liquid hydrogen target installed in the geometrical center of the Crystal Ball were used to search for  $\omega \rightarrow \eta\pi^0$ . The events were reconstructed from the pool of five-cluster events which include four photons and one proton cluster. Both, Crystal Ball and TAPS clusters were used in the analysis. A CB cluster included the central crystal (the crystal with the maximum deposited energy) and up to 22 surrounding crystals with energies above 1.1 MeV. The energy in the central crystal was required to be above 15 MeV. A TAPS cluster was constructed from the central crystal, which has a minimum energy of 20 MeV, plus up to 18 surrounding detectors with energies 3.5 MeV or higher. The timing information for each crystal was used to ensure that all the hits in a cluster originate from the same particle. The timing coincidence window for the Crystal Ball was set to 70 ns, and for TAPS it was 30 ns. The typical time resolution for the Crystal Ball is ≈6 ns (FWHM). A time resolution of 160 ps was achieved for the TAPS detector [12]. The energy of a photon cluster, calculated as the sum of the energies deposited in all crystals contributing to the cluster, was corrected for the leakage of the electromagnetic shower outside of the cluster boundaries and for nonlinearity of the analog-to-digital converters. The energy-dependent corrections were calculated from a Monte Carlo simulation and verified using the experimental data. For the case of the proton cluster, only the angular information was used in the kinematical fit.

The event candidates were subjected to a fit with kinematical constraints [14]. All combinations of five clusters were

tested for the  $\gamma p \rightarrow \eta\pi^0 p$  hypothesis with the  $\eta$  and the  $\pi^0$  decaying to two photons. An event with  $n$  hits in the beam tagger was treated as  $n$  independent events with beam energies  $E_n$ . The event was selected for further analysis if at least one combination of clusters satisfied the  $\gamma p \rightarrow \eta\pi^0 p$  hypothesis at the 95% confidence level (C.L.), i.e., with probability greater than 5%. The cut on the probability was optimized in order to minimize the combinatorial background which is estimated to be less than 4%. The selected events included ≈5% contamination from the random beam background. This background was determined using the random hits in the beam tagger and subtracted. Only the interval in the photon bremsstrahlung spectrum from  $E_\gamma = 1.171$  GeV to 1.322 GeV was used for the analysis in order to maximize the ratio of the production cross sections  $\sigma_{\text{total}}(\gamma p \rightarrow \omega p)$  to  $\sigma_{\text{total}}(\gamma p \rightarrow \eta\pi^0 p)$ . The ratio was further improved by applying an additional two-dimensional cut on the  $\gamma p \rightarrow \eta\pi^0 p$  Dalitz plot, see Fig. 1. The Dalitz plot indicates an enhancement at  $M^2(\eta p) \approx 2.31$  (GeV/c<sup>2</sup>)<sup>2</sup> and  $M^2(\pi^0 p) \approx 1.44$  (GeV/c<sup>2</sup>)<sup>2</sup> reflecting the complex dynamics of the  $\gamma p \rightarrow \eta\pi^0 p$  reaction. The applied cut removes the enhancement reducing the number of the background  $\eta\pi^0$  events in the  $\omega$  mass region by about factor of four, see Fig. 1(c). The cut reduces the acceptance of  $\gamma p \rightarrow \omega(\eta\pi^0)p$  by about 70%. The resulting distribution of the  $\eta\pi^0$  invariant mass in the region of the  $\omega$  mass is shown in Fig. 2 and compared to the Monte Carlo simulation of  $\gamma p \rightarrow \omega(\eta\pi^0)p$ . The simulated acceptance depends on the beam energy. The average acceptance is about 11%. The  $\eta\pi^0$  invariant mass, constrained by momentum and energy conservation and by the masses of the  $\eta$  and the  $\pi^0$ , has a width of  $\sigma \approx 14$  MeV. This width is a combination of the detector resolution (≈8.5 MeV) and the simulated  $\omega$  width of 8.49 MeV [3]. The Monte Carlo sample of  $\gamma p \rightarrow \omega p$  events was generated according to the  $\omega$  angular distribution determined from our data. The invariant mass interval from 740 MeV to 830 MeV was used to calculate the upper limit for the number of  $\omega \rightarrow \eta\pi^0$  events. The spectrum was fitted with a combination of a linear function plus a Gaussian. Only the normalization constant of the Gaussian, const., was a variable of the fit. The mean value and the sigma were fixed to the values determined from the Monte Carlo simulation.

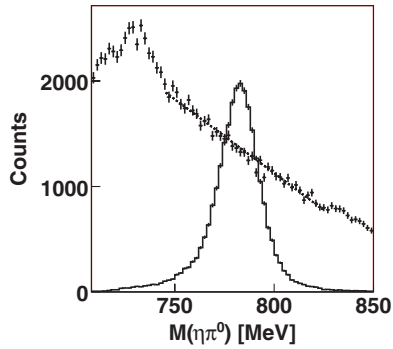


FIG. 2. Invariant mass spectrum of  $\eta\pi^0$  in the region of the  $\omega$  mass. The points with the error bars show the experimental data and the solid line is the Monte Carlo simulation of  $\omega \rightarrow \eta\pi^0$ . The  $\eta$ 's were detected using the  $\eta \rightarrow \gamma\gamma$  mode. The dashed line shows the results of the fit to the combination of a linear function plus a Gaussian used to determine the number of  $\omega \rightarrow \eta\pi^0$  events. The lack of smoothness in the mass distribution is the consequence of our technique for removing the process  $\gamma p \rightarrow \eta\pi^0 p$ , which is the major background reaction to the  $\omega \rightarrow \eta\pi^0$  decay.

The constant was constrained to have only positive values. A Gaussian function was constructed with the mean and the sigma determined from the simulation and the normalization constant equal to

$$\text{const.} = \text{const.}_{\text{fit}} + 1.644 \times \sigma(\text{const.}_{\text{fit}}), \quad (1)$$

where  $\text{const.}_{\text{fit}}$  is the normalization constant as calculated by the fit, and  $\sigma(\text{const.}_{\text{fit}})$  is the uncertainty for the  $\text{const.}_{\text{fit}}$  from the fit. The interval of  $1.644\sigma$  provides the 90% confidence level for the probability distribution in the form of a Gaussian limited to positive values with the mean value close to zero. The upper limit to the number of the  $\omega \rightarrow \eta\pi^0$  events was calculated as the integral of the Gaussian distribution in the  $\pm 2\sigma$  range. The upper limit to the number of  $\omega \rightarrow \eta(2\gamma)\pi^0$  events in Fig. 2 is 60 events, or 1385 events after correction to the experimental acceptance and the  $BR(\eta \rightarrow \gamma\gamma) = 0.39$  [3].

The upper limit for the branching ratio of the  $\omega \rightarrow \eta\pi^0$  decay was calculated with respect to the number of  $\omega \rightarrow \pi^0\gamma$  events produced in the beam energy interval  $E_\gamma = 1.171\text{--}1.322$  GeV and corrected for the  $BR(\omega \rightarrow \pi^0\gamma) = 0.0892$  [3]. The  $\gamma p \rightarrow \pi^0\gamma p$  events were reconstructed from four-cluster events: three photons and the proton. All combinations of clusters and the beam tagger hits were tried for the  $\gamma p \rightarrow \pi^0\gamma p$  hypothesis to find the best combination. The  $\pi^0\gamma$  invariant mass in the  $\omega$  region is shown on Fig. 3 compared to results of the simulation. The total number of  $\omega$  produced in the beam energy interval  $E_\gamma = 1.171\text{--}1.322$  GeV is  $6.1 \times 10^6$ . From this number the upper limit for the branching ratio of  $\omega \rightarrow \eta\pi^0$  is calculated to be

$$BR(\omega \rightarrow \eta\pi^0) < 2.3 \times 10^{-4} \text{ at C.L.} = 90\%. \quad (2)$$

Using a similar technique, we also calculated the upper limits for two other forbidden  $\omega$  decays. The upper limits for  $BR(\omega \rightarrow 3\pi^0)$  and  $BR(\omega \rightarrow 2\pi^0)$  were calculated for the beam energy range 1.203 GeV to 1.403 GeV covering the maximum of the  $\omega$  photoproduction cross section at

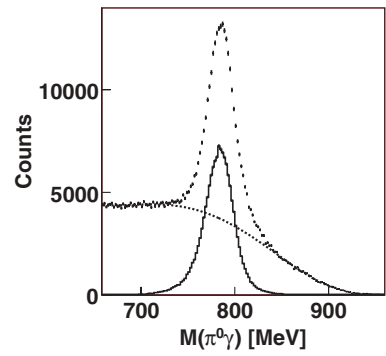


FIG. 3. Invariant mass spectrum of  $\pi^0\gamma$  obtained for the reaction  $\gamma p \rightarrow \pi^0\gamma p$ . The peaks in the spectra correspond to the decay  $\omega \rightarrow \pi^0\gamma$ . The data (points with error bars) are compared to the Monte Carlo simulation (solid line). The total number of events in the experimental peak is about  $1.5 \times 10^5$ . The smooth background under the  $\omega \rightarrow \pi^0\gamma$  peak comes from the  $2\pi^0$  production.

the MAMI-C tagged photon beam energies. The major background for the decay  $\omega \rightarrow 2\pi^0$  is  $\gamma p \rightarrow 2\pi^0 p$ . The total cross section of  $\gamma p \rightarrow 2\pi^0 p$  decreases steadily between 1.203 GeV and 1.403 GeV photon beam energy [15]. Therefore the choice of the beam range maximizes the  $\sigma_{\text{total}}(\gamma p \rightarrow \omega p)$  to  $\sigma_{\text{total}}(\gamma p \rightarrow \pi^0\pi^0 p)$  ratio. For the  $\omega \rightarrow 3\pi^0$  decay the main background is the  $\gamma p \rightarrow 3\pi^0 p$  direct production. There is no existing data on the total cross section of this reaction. The fitting function was constructed from a second-order polynomial plus a Gaussian. The total number of the  $\gamma p \rightarrow \omega p$  events in this interval, calculated from the number of detected  $\omega \rightarrow \pi^0\gamma$  decays, is  $7.2 \times 10^6$ . The resulting upper limits are

$$BR(\omega \rightarrow 3\pi^0) < 2.3 \times 10^{-4} \text{ at C.L.} = 90\% \quad (3)$$

and

$$BR(\omega \rightarrow 2\pi^0) < 2.4 \times 10^{-4} \text{ at C.L.} = 90\%. \quad (4)$$

The values of the acceptance used are 13% for  $\omega \rightarrow 3\pi^0$  and 19% for  $\omega \rightarrow 2\pi^0$ . The distributions of the invariant mass for  $3\pi^0$  from  $\gamma p \rightarrow 3\pi^0 p$  and  $2\pi^0$  from  $\gamma p \rightarrow 2\pi^0 p$  in the region of the  $\omega$  mass are shown in Fig. 4 compared to the

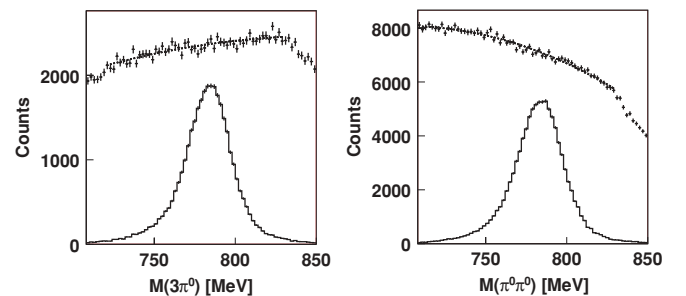


FIG. 4. The left figure shows the invariant mass of the  $3\pi^0$  final state in the region of the  $\omega$  mass. The points with the error bars show the experimental data and the solid line is the Monte Carlo simulation of  $\omega \rightarrow 3\pi^0$ . The dashed line shows the results of the fit to the combination of a second-order polynomial plus a Gaussian. The fit was used to determine the number of  $\omega \rightarrow 3\pi^0$  events. The right figure shows the same for the  $2\pi^0$  final state.

TABLE I. Inputs for the calculation of the upper limits  $\omega \rightarrow \eta\pi^0$ ,  $\omega \rightarrow 3\pi^0$ , and  $\omega \rightarrow 2\pi^0$ . For the  $\omega \rightarrow \eta\pi^0$  decay the number of  $\omega \rightarrow \pi^0\gamma$  was calculated for the beam interval of  $1.171 < E_{\text{beam}} < 1.322$  GeV. For the other two decay modes the beam interval was  $1.203 < E_{\text{beam}} < 1.403$  GeV.

	$N_{\text{events meas.}}$	Accept.	$N_{\text{events total}}$	BR u.l.
$\omega \rightarrow \pi^0\gamma$	$1.42 \times 10^5$	0.26		
$\omega \rightarrow \text{all}$			$6.1 \times 10^6$	
$\omega \rightarrow \eta(\gamma\gamma)\pi^0$	$<60$	0.11		
$\omega \rightarrow \eta\pi^0$			$<1385$	$<2.3 \times 10^{-4}$
$\omega \rightarrow \pi^0\gamma$	$1.76 \times 10^5$	0.27		
$\omega \rightarrow \text{all}$			$7.3 \times 10^6$	
$\omega \rightarrow 3\pi^0$	$<219$	0.13	$<1685$	$<2.3 \times 10^{-4}$
$\omega \rightarrow 2\pi^0$	$<336$	0.19	$<1768$	$<2.4 \times 10^{-4}$

Monte Carlo results. All the numerical values used for the calculation of the upper limits are summarized in Table I.

The ratio  $BR(\omega \rightarrow 3\pi^0)/BR(\omega \rightarrow \pi^+\pi^-\pi^0) \leq (2 \times 10^{-4})/0.891 = 1.2 \times 10^{-4}$  gives an estimate of the sensitivity of the  $\omega \rightarrow 3\pi^0$  decay to the  $C$  violating amplitude. The decay  $\omega \rightarrow 2\pi^0$  can be compared to the allowed decay  $\rho \rightarrow \pi^+\pi^- : \Gamma(\omega \rightarrow \pi^0\pi^0)/\Gamma(\rho \rightarrow \pi^+\pi^-) \leq (2 \times 10^{-4} \times 8.49)/150 = 1.1 \times 10^{-5}$ . Finally, we can compare  $\omega \rightarrow \eta\pi^0$  to  $a_0(980) \rightarrow \eta\pi^0$  which is the dominant decay mode with  $\Gamma \approx 50\text{--}100$  MeV. Thus  $\Gamma(\omega \rightarrow \eta\pi^0)/\Gamma(a_0(980) \rightarrow \eta\pi^0) \leq (2 \times 10^{-4} \times 8.49)/75 = 2.2 \times 10^{-5}$ .

The authors very much appreciate the dedicated work of the MAMI accelerator group. We also thank the undergraduate students of Mount Allison University and the George Washington University for their assistance in data taking. This work was supported by the US DOE and US NSF, EPSRC and STFC of the UK, NSERC of Canada, the Deutsche Forschungsgemeinschaft (SFB 443) of Germany, and DFG-RFBR (Grant No. 09-02-91330) of Germany and Russia, SNF of Switzerland, and the European Community-Research Infrastructure Activity under the FP6 ‘‘Structuring the European Research Area’’ program (Hadron Physics, Contract No. RII3-CT-2004-506078).

- 
- [1] A. D. Sakharov, *Sov. Phys. Jour. of Exp. and Theor. Phys.* **5**, 24 (1967).  
[2] B. M. K. Nefkens *et al.*, *Phys. Rev. Lett.* **94**, 041601 (2005).  
[3] C. Amsler *et al.* (Particle Data Group), *Phys. Lett.* **B667**, 1 (2008).  
[4] D. Alde *et al.*, *Phys. Lett.* **B340**, 122 (1994).  
[5] Y. D. Prokoshkin and V. D. Samoilenko, *Sov. Phys. Dokl.* **40**, 273 (1995).  
[6] I. Anthony *et al.*, *Nucl. Instrum. Methods A* **301**, 230 (1991).  
[7] S. J. Hall *et al.*, *Nucl. Instrum. Methods A* **368**, 698 (1996).  
[8] J. C. McGeorge *et al.*, *Eur. Phys. J. A* **37**, 129 (2008).  
[9] A. Starostin *et al.*, *Phys. Rev. C* **64**, 055205 (2001).  
[10] S. Prakhov *et al.*, *Phys. Rev. C* **78**, 015206 (2008).  
[11] C. M. Tarbert *et al.*, *Phys. Rev. Lett.* **100**, 132301 (2008).  
[12] R. Novotny, *IEEE Trans. Nucl. Sci.* **38**, 379 (1991).  
[13] R. Gabler *et al.*, *Nucl. Instrum. Methods A* **346**, 168 (1994).  
[14] V. Blobel, documentation and source are available at <http://www.desy.de/~blobel/>.  
[15] A. V. Sarantsev *et al.*, *Phys. Lett.* **B659**, 94 (2008).